*Journal of Experimental Botany*, Vol. 63, No. 13, pp. 4781–4795, 2012
doi:10.1093/jxb/ers156
This paper is available online free of all access charges (see http://jxb.oxfordjournals.org/open_access.html for further details)

Journal of Experimental Botany
www.jxb.oxfordjournals.org

**RESEARCH PAPER**

# Antisense reductions in the PsbO protein of photosystem II leads to decreased quantum yield but similar maximal photosynthetic rates

**Simon A. Dwyer, Wah Soon Chow, Wataru Yamori, John R. Evans, Sarah Kaines, Murray R. Badger and Susanne von Caemmerer***

Research School of Biology, The Australian National University, Canberra ACT 0200, Australia

* To whom correspondence should be addressed: E-mail: susanne.caemmerer@anu.edu.au

Received 8 March 2012; Revised 26 April 2012; Accepted 30 April 2012

## Abstract

**Photosystem (PS) II is the multisubunit complex which uses light energy to split water, providing the reducing equivalents needed for photosynthesis. The complex is susceptible to damage from environmental stresses such as excess excitation energy and high temperature. This research investigated the *in vivo* photosynthetic consequences of impairments to PSII in *Arabidopsis thaliana* (ecotype Columbia) expressing an antisense construct to the PsbO proteins of PSII. Transgenic lines were obtained with between 25 and 60% of wild-type (WT) total PsbO protein content, with the PsbO1 isoform being more strongly reduced than PsbO2. These changes coincided with a decrease in functional PSII content. Low PsbO (less than 50% WT) plants grew more slowly and had lower chlorophyll content per leaf area. There was no change in content per unit area of cytochrome $b_6f$, ATP synthase, or Rubisco, whereas PSI decreased in proportion to the reduction in chlorophyll content. The irradiance response of photosynthetic oxygen evolution showed that low PsbO plants had a reduced quantum yield, but matched the oxygen evolution rates of WT plants at saturating irradiance. It is suggested that these plants had a smaller pool of PSII centres, which are inefficiently connected to antenna pigments resulting in reduced photochemical efficiency.**

**Key words:** Arabidopsis, chlorophyll fluorescence, oxygen evolution, photosynthesis, photosystem II, PsbO.

## Introduction

Primary carbon fixation in plants requires the coordination of the photosynthetic carbon reduction (PCR) cycle and the light-dependent thylakoid reactions, with each process featuring a number of enzymatic steps (Kramer and Evans, 2011). The thylakoid-bound photosystem (PS) II complex features the molecular framework and high redox potential needed to oxidize water, the source of the available electrons, and protons required for nearly all carbon fixation on Earth, with the by-product of molecular oxygen providing the atmosphere that allows for aerobic respiration (Satoh, 1996; Barber, 2006). In concert with the other thylakoid-bound photosynthetic complexes, water splitting by PSII converts absorbed light energy into the reducing equivalents required by the PCR cycle to fix $CO_2$ into stable sugars via the $CO_2$-fixing enzyme Rubisco (Barber, 2006; Kramer and Evans, 2011).

During steady-state photosynthesis by healthy leaves, photosynthetic rate will usually be limited either by $CO_2$ fixation by Rubisco (e.g. at high light or low $CO_2$) or by the rate of energy production from the thylakoid reactions (e.g. at low light or high $CO_2$) (Farquhar *et al.*, 1980; von Caemmerer and Farquhar, 1981; von Caemmerer, 2000). Water-splitting and subsequent electron donation by PSII is rarely considered a rate limiting step to the thylakoid reactions in non-stressed leaves (Evans, 1988; Makino

et al., 1994; Price et al., 1998; Yamori et al., 2010). However under stressed conditions such as excessive light or high temperature, PSII is the more labile of the thylakoid complexes (Berry and Björkman, 1980; Long et al., 1994; Murata et al., 2007; Tyystjärvi, 2008; Takahashi and Badger, 2011). The fragility and dynamic changes of the complex are considered a consequence of the effects of UV and blue light on the water splitting complex, the high redox potentials necessary to oxidize water and the sensitivity of the protein repair system to reactive oxygen species (Andersson et al., 1992; van Gorkom and Schelvis, 1993; Takahashi and Murata, 2008; Oguchi et al., 2011; Takahashi and Badger, 2011). The chloroplast encoded D1 protein which, along with the D2 protein, forms the core of PSII, undergoes a constant cycle of oxidative damage, degradation, and replacement, and even under non-stressed conditions has a half life of just 2 h (Ohad et al., 1984; Greer et al., 1986; Andersson et al., 1992; Sundby et al., 1993; Andersson and Barber, 1996; Yamashita et al., 2008). Loss of PSII function through these mechanisms can be associated with reduced photosynthetic rates (Ohad et al., 1984; Long et al., 1994). For example in capsicum leaves, it has been demonstrated that photoinhibition of 40% of the total PSII pool can cause a decline in maximum photosynthetic rate at high light (Lee et al., 1999). Under low light conditions, PSII may set the rate of thylakoid electron transport, and consequently influences carbon fixation, primary productivity, and crop yield (Farage and Long, 1991; Long et al., 1992, 1994; Stirling et al., 1993).

Of the eight PSII subunits which are nuclear encoded in *Arabidopsis thaliana*, and hence relatively easy to genetically manipulate, the extrinsic PsbO protein is one of the most important (Bricker, 1992; Kuwabara and Murata, 1983; Mayfield et al., 1987b; Wollman et al., 1999). The protein, often referred to as the 33 kDa protein or the manganese stabilizing protein (MSP), is highly conserved across oxygenic photosynthetic organisms, from cyanobacteria to angiosperms, which in itself suggests a critical role for PSII function (Bricker and Frankel, 1998; Leuschner and Bricker, 1996). The subunit is exposed to the lumenal side of the thylakoid membrane and plays a functional role at the water splitting site, in addition to a structural role, interacting with several of the core PSII subunits (Barber, 2006). Impaired or absent PSII function has been shown in PsbO-lacking mutants in organisms as diverse as *Synechocystis* (sp. PCC6803, Burnap and Sherman, 1991), *Chlamydomonas reinhardtii* (Mayfield et al., 1987a, 1987b) and *A. thaliana* (Yi et al., 2005). These important roles and interactions made the PsbO protein an ideal target for antisense reductions for the purposes of this study.

In *A. thaliana* there are two regions of nuclear DNA encoding two distinct isoforms of the PsbO protein, PsbO1 and PsbO2 (encoded by At5g66570 and At3g50820, respectively, the Arabidopsis Information Resource, http://www.arabidopsis.org) with the PsbO1 isoform being far more abundant (Murakami et al., 2002). Though the cDNA sequences for the two genes are 83% similar in the coding region, a separate role for the two isoforms was predicted from the assumption that natural selection would be unlikely to maintain a superfluous gene/protein and this has been supported by empirical evidence (Murakami et al., 2002; Lundin et al., 2007). Gene knock-out experiments have indicated that the two isoforms appear to have different roles in water splitting and the phosphorylation and degradation of the D1 protein and subsequent repair of the PSII complex (Lundin et al., 2007, 2008; Allahverdiyeva et al., 2009). PsbO1 appears to play a role in the association of the calcium ion cofactor at the water splitting site, thereby enhancing PSII activity, whereas PsbO2 is more important for the degradation and turnover of the D1 subunit that is necessary to maintain active PSII complexes (Lundin et al., 2007, 2008; Bricker and Frankel, 2008; Allahverdiyeva et al., 2009).

This study aimed to investigate how PSII limits overall photosynthetic rate and interacts with other photosynthetic components by using antisense RNA technology to change the stoichiometry of PSII *in vivo*. Antisense studies have been used successfully to investigate aspects of the PCR cycle (Raines, 2003) and aspects of the light-dependent thylakoid reactions, for example cytochrome $b_6f$ (Price et al., 1998, 1995), PSI (Haldrup et al., 2003) and ATP synthase (Price et al., 1995; Rott et al., 2011; Yamori et al., 2011b). Decreasing leaf cytochrome $b_6f$ content by antisense reductions in the Rieske FeS protein decreased chloroplast electron transport rate proportionally (Price et al., 1995, 1998; Anderson et al., 1997; Ruuska et al., 2000; Yamori et al., 2011b), confirming early measurements that indicated a direct link between cytochrome $b_6f$ content and maximum chloroplast electron transport capacity (Evans, 1987a, 1988). ATP synthase also exerts a significant limitation on electron transport rate (Price et al., 1995) but this is alleviated somewhat by the ability of the complex to increase its activity *in vivo* (Kanazawa and Kramer, 2002; Kramer et al., 2004a; Rott et al., 2011; Yamori et al., 2011a). Only a few studies have used antisense techniques to examine the effects on photosynthesis when PSII capacity is diminished (Stockhaus et al., 1990; Andersson et al., 2001; García-Cerdán et al., 2009). This study reports on the *in vivo* photosynthetic consequences of impairing the capacity of PSII in leaves through antisense reductions in the PsbO proteins in *A. thaliana*.

## Materials and methods

### *Plasmid construction and generation of transgenic plants*

*A. thaliana* (ecotype Columbia) RNA was extracted in TRIzol reagent (Invitrogen, Australia) and cDNA was synthesized. A segment of *psbO1* was amplified with the primer pair 5′-CACCCTCAAGTTGACCATACCACA-3′ (forward) and 5′-GTGGCCATGGCAGCCTCTCT-3′ (reverse) using Platinum Pfx DNA polymerase (Invitrogen). The 1006-bp product spans the full length of the coding DNA sequence of *psbO1* and was intended to also affect *psbO2*, which has an 81% similar coding sequence. A BLAST of the reverse complement of the antisense product, for both coding regions and 5′- and 3′ untranscribed regions for *A. thaliana*, found a maximum complementarity with other genes of just 20 bp (Altschul et al., 1997), less than generally required for RNA suppression (Huntzinger and Izaurralde, 2011). The PCR product was purified from an agarose gel and cloned into the pENTR vector, transformed into *Escherichia coli* TOP10 (Invitrogen) and sequences confirmed. A Gateway LR Clonase II enzyme mix reaction was used to transfer the construct to the Gateway binary vector, pMDC32 cassette C1 (Curtis and Grossniklaus, 2003) and transformed into *Agrobacterium tumefaciens* AGL1 (Lazo et al., 1991). The gene construct was transferred into *A. thaliana* (ecotype Columbia) using the floral dip method described by Clough and Bent (1998).

T1 seed was screened for hygromycin resistance on Murashige and Skoog Basal medium (Murashige and Skoog, 1962), with 0.8% (w/v) Bacto agar (BD, France), 3% (w/v) sucrose, 30 μg/ml (w/v) hygromycin (Sigma-Aldrich, Australia), and 150 μg/ml (w/v) timentin (GlaxoSmith-Kline, Australia). Seed was stratified at 4 °C for 48 h then germinated in conditions of 25 °C and 18/6 h light/dark cycle with an irradiance of

100–150 μmol quanta $m^{-2}$ $s^{-1}$ provided by fluorescent lights. Resistant plants were selected by fully expanded cotyledons in the first few days and the development of true leaves within a week.

A number of hygromycin-resistant T1 plants were identified and these were transferred to soil and grown to seed for analysis of the T2 generation. Second-generation (T2) plant lines were identified by a number corresponding to their T1 parent, such that all plants with a different line number are the progeny of independent T1 transformants.

### *Plant growth conditions*

Second-generation (T2) transgenic lines were germinated similarly to T1 seed, but without hygromycin or timentin. After approximately 10 days, when at least two true leaves had developed, plants were transferred to soil supplemented with slow release fertilizer (Osmocote Exact, Scotts, Australia), and moved to a controlled environment growth chamber. Photoperiod was 9 h, relative humidity 70%, irradiance at pot height 200 μmol quanta $m^{-2}$ $s^{-1}$ and day/night temperature was 23/18 °C.

### *Plant growth rates*

The top view photosynthetic ground cover was used as a proxy for plant size, determined by a chlorophyll fluorescence imaging system (CF Imager, Technologia, UK; Oxborough and Baker, 1997a). This method will increasingly underestimate leaf area with time due to increasing leaf overlap, but was convenient and non-destructive. Area measurements started 10 days after plants were transferred to soil (after 14 days on germination media). Area was then measured every 3 days. Relative rate of rosette area increase over the course of the experiment was calculated by fitting an exponential to the increase in area of each individual plant over the course of measurements.

### *Determination of leaf functional PSII, cytochrome f, Rubisco, and chlorophyll content*

The leaf content of functional PSII centres was determined from the oxygen yield per single turnover saturating flash on fresh leaf discs in 1% $CO_2$ in an oxygen electrode chamber (LD2/3 chamber with an S1 silver-platinum electrode disc, Hansatech, Norfolk, England), according to Chow *et al.* (1989, 1991). The oxygen yield per flash was used to calculate the number of functional (oxygen evolving) PSII centres per leaf area, assuming one oxygen molecule is evolved from each PSII centre per four flashes.

Total Rubisco catalytic sites per leaf area were quantified by the stoichiometric binding of the radioactively labelled inhibitor, [$^{14}$C] carboxyarabinitol-bisphosphate (CABP), according to the method described in Ruuska *et al.* (1998).

Leaf cytochrome *f* content was determined on a pooled thylakoid sample from WT plants only, extracted as per Dwyer *et al.* (2007). Cytochrome *f* concentration was calculated from the spectra of the hydroquinol-reduced, relative to ferricyanide-oxidized, solution, according to Bendall *et al.* (1971).

For leaf chlorophyll content, frozen leaf samples were ground in phosphate-buffered 80% acetone (pH 7.8) then chlorophyll *a* and *b* concentration determined from absorbance readings at 646.6, 663.6, and 750 nm in a Cary 50 Bio UV-visible spectrophotometer (Varian, USA), according to Porra *et al.* (1989).

### *Western blotting*

Leaf content of PsbO and other photosynthetic proteins was determined on an area basis through Western blotting relative to a four-point (25, 50, 75, and 100%) dilution series of a WT leaf extract according to Yamori *et al.* (2011b) with some modifications. The same WT extract was used as a standard for all quantifications and the mean coefficient of determination ($r^2$) for the standard curves used for protein quantification was 0.996 ± 0.002. Primary antibodies for the photosynthetic proteins PsbO, PsbD, PetC, PsaD, and AtpC were sourced from Agrisera (Vännäs, Sweden).

To visualize the two PsbO isoforms, thylakoids were isolated as for cytochrome *f* measurements, except that individual plant samples were not pooled. Thylakoid samples were denatured by boiling for 5 min in loading buffer (250 mM TRIS-HCl, pH 8.5, 10% (v/v) glycerol, 2% (w/v) SDS, 0.5 mM EDTA, 0.01% (w/v) bromophenol blue, and 5% (v/v) beta-mercaptoethanol). Denatured samples were loaded on a chlorophyll basis, equivalent to 2 μg chlorophyll, and separated on a precast 18% TRIS-glycine gel (Invitrogen). Proteins were transferred and visualized as described above using the same PsbO primary antibody.

### *Blue native PAGE*

Thylakoid samples were isolated as described above for cytochrome *f* measurement. Membrane suspensions were solubilized on ice with the addition of n-dodecyl-β-D-maltoside (Sigma-Aldrich) to a final concentration of 2% and insoluble material removed by centrifugation at 12,000 *g* for 10 min at 4 °C. A 1/10 volume of loading buffer of 100 mM BIS-TRIS-HCl (pH 7.0), 500 mM 6-aminocaproic acid, 30% (v/v) glycerol, and 5% (w/v) Serva Blue G (SERVA Electrophoresis, Germany) was added to the mixture. Thylakoid solutions equivalent to 4 μg chlorophyll were loaded on a 4–16% gradient Novex NativePAGE BIS-TRIS gel (Invitrogen) at 4 °C with the running voltage increased from 75 V to 200 V over the course of the 3-h run. The cathode buffer (15 mM BIS-TRIS, 50 mM Tricine-HCl, pH 7.0) with 0.1% (w/v) SERVA Blue G was exchanged for a dye-free buffer after the dye front was two-thirds of the way down the gel. After running, the gel was scanned, stained with GelCode Blue Stain Reagent (ThermoScientific, USA), then scanned again. Bands were identified according to Järvi *et al.* (2011) and quantified using the Quantity One software (v 4.6.3, Bio-Rad, USA).

### *Chlorophyll a fluorescence measurements*

The maximum quantum yield of PSII photochemistry measured by the chlorophyll *a* fluorescence ratio, $F_V/F_M$, was determined using a PAM-101 fluorometer (Walz, Effeltrich, Germany) with a red measuring beam and fluorescence detection at wavelengths greater than 710 nm. Saturating flashes of 1 s duration were provided by a halogen flash lamp (150 W) at an intensity of 5000 μmol quanta $m^{-2}$ $s^{-1}$. Plants were dark acclimated for a minimum of 2 h.

### *P700 measurements*

Redox changes in P700 were monitored through absorbance changes at 810 nm (relative to a reference wavelength of 870 nm to control for plastocyanin and other signal contamination) under saturating single turnover flashes superimposed over steady far red light, as described in Losciale *et al.* (2008) with the exception that the signal was calibrated by a signal change corresponding to 0.1% change in transmission under steady-state far red light to yield a (calibrated) change in transmittance, $\triangle T_c$. This signal was then converted to absorbance units, $\triangle A$, according to the Beer–Lambert law, $\triangle A = \log_{10}(1 + \triangle T_c)$ (see Supplementary Methods for derivation, available at *JXB* online).The value of $\triangle A$ is directly proportional to the concentration of $P700^+$ and the maximum absorbance achieved immediately after the saturating flash, $\triangle A_{max}$, is proportional to the total amount of photo-oxidizable P700, assuming the measuring beam path length remains relatively constant.

### *Leaf absorbance and response of oxygen evolution to irradiance*

Oxygen evolution rates were measured on leaf discs in a water-jacketed (23 °C) gas-phase oxygen electrode chamber (LD2/3 chamber with an S1 silver-platinum electrode disc, Hansatech, England), the top window of which was modified for insertion of a 4 $cm^2$ fibre optic bundle which provided actinic light and allowed measurement of chlorophyll fluorescence via the Walz PAM 101 system described above. Actinic light was provided by a 100 W xenon projector lamp with an infrared filter, with intensity controlled by neutral density filters. The spectrum of this source, measured with a spectroradiometer (LI-1800, LI-COR, USA), showed a peak intensity at 590 nm, and intensity at wavelengths greater than 700 nm was 15% of that between 400 and

700 nm. The absorbance of each leaf measured was determined with a spectroradiometer and leaf integrating sphere (LI-1800-12).

Leaf pieces of approximately 3 $cm^2$ were placed into the darkened oxygen electrode chamber with a pad dampened with 1M $NaHCO_3$ (pH 9) to provide a $CO_2$ concentration of approximately 10 mmol $mol^{-1}$ (Chow *et al.*, 1989). The oxygen electrode was calibrated by injecting 1 ml of air into the chamber then allowed to stabilize for 5 min. The slope of the electrode voltage over time in the dark was taken to be the baseline associated with mitochondrial respiration and any instrumental drift, and all gross oxygen evolution rates were determined relative to it. Irradiance was increased stepwise to the maximum, allowing 5 min for stabilization at each of the following incident irradiances: 0, 25, 50, 115, 200, 300, 430, 500, 800, 1000, and 1450 µmol quanta $m^{-2}$ $s^{-1}$. Quantum yields were calculated from the average increase in oxygen evolution per absorbed quanta between 0 and 115 µmol quanta $m^{-2}$ $s^{-1}$ incident irradiance. Maximum oxygen evolution rates were determined from the average of the rate measured at the three highest incident light irradiances, 800, 1000, and 1450 µmol quanta $m^{-2}$ $s^{-1}$. Gross oxygen evolution rates ($E_{ogross}$) were fit to the following empirical model (Ögren and Evans, 1993; von Caemmerer, 2000):

$$E_{0gross} = \frac{\Phi_0 I_{abs} + E_{0\max} - \sqrt{(\Phi_0[I_{abs} + E_{0\max})]^2 - 4\theta\ \Phi_0 I_{abs} E_{0\max}}}{2\theta} \quad (1)$$

where $E_{Omax}$ is the maximum gross oxygen evolution rate, $I_{abs}$ the irradiance absorbed by the leaf and θ the curvature factor. The leaf quantum yield for oxygen evolution, $\Phi_O$, is dependent on both the intrinsic PSII quantum efficiency and the distribution of excitation energy between PSII and PSI, *X*. The model was fitted using the least squares method to find values for $E_{Omax}$, θ, and $\Phi_O$.

Linear chloroplast electron transport rate from PSII calculated from chlorophyll fluorescence, $J_f$, is given by:

$$J_f = \Phi_{PSII} \times I_{abs} \times X \quad (2)$$

where $\Phi_{PSII}$ is the quantum yield from chlorophyll fluorescence (Genty *et al.*, 1989) and *X* is the ratio of quanta absorbed by PSII to quanta absorbed by the leaf (Maxwell and Johnson, 2000).

By substituting the linear electron transport rate calculated from oxygen evolution (assuming four electrons per molecular oxygen), $J_{oxygen}$, for $J_f$ and rearranging Equation 2, an estimate of the partitioning of quanta to PSII can be obtained from the combination of chlorophyll fluorescence and oxygen electrode measurements:

$$X = \frac{J_{oxygen}}{\Phi_{PSII} \times I_{abs}} \quad (3)$$

This calculation for *X* is a comparison between electron transport rates calculated from oxygen evolution and from chlorophyll fluorescence.

### *Microscopy*

Representative leaves were cut into pieces of approximately 1–2 × 3–4 mm and embedded in Araldyte 502 similarly to the method of Pengelly *et al.* (2010). Sections for light microscopy were cut from embedded leaf pieces at 0.5 mm thickness using glass knives on an ultramicrotome (Ultracut E, Leica, Austria), stained with toluidine blue, and heat-fixed to glass slides. Sections were viewed through light microscope (Axioskop, Zeiss, Germany) and images captured on a high-resolution CCD camera (Flex, Spot Imaging, USA). Chloroplast number per palisade cell and number of cell layers were counted manually for three regions per section, using ×200 and ×400 magnification respectively. Leaf thickness was determined on three regions per ×200 image using ImageJ software (NIH, USA). These measurements were repeated on three independent leaves for both WT and low PsbO plants. The average value per section was used for statistical analysis.

Thin sections of approximately 90 nm were cut from the upper palisade layer of leaves using an ultramicrotome and stained with uranyl acetate and lead citrate. The sections were viewed in a transmission electron microscope (H7000, Hitachi, USA) at 75 kV and digital images captured with a CCD camera (13C, Scientific Instruments and Applications, USA).

### *Statistical treatments*

Linear and non-linear relationships were fit in Origin (v7.03, OriginLab Corporation, USA) using a least-squares method with a chi-squared tolerance of $5 \times 10^{-50}$. Correlation coefficients and Student's t-tests were calculated performed using Statistica (v6.0, StatSoft, USA).

## Results

### *Anti-*psbO *phenotype*

Total leaf PsbO protein content of T2 progeny of transgenic PsbO antisense lines was determined from band intensity on a Western blot relative to a dilution series of a standard extract from wild-type plants. Wild-type (WT) leaves varied in PsbO content from 60 to 130% of the reference extract (Fig. 1). Transgenic T2 lines exhibited a wider range, down to approximately 25% in lines 8 and 15. Functional (i.e. oxygen producing) PSII content, determined on fresh leaf discs from the oxygen yield per single turnover flash method, decreased almost in direct proportion with decreasing PsbO content (Fig. 1A). Photosystem II content in the lowest transgenic plants measured was around 0.3 µmol $m^{-2}$, approximately 27% of that measured in WT plants.

High-resolution gel electrophoresis and immunoblotting was performed separately to the above-mentioned Western blots to determine the relative change in the amount of the two PsbO isoforms in the plants with lowest PsbO contents (Fig. 1B). The antisense effect was most evident on the PsbO1 isoform compared to PsbO2. The proportion of the total PsbO content accounted for by the PsbO1 isoform was reduced from 59 to 43% ($P = 0.0001$, Fig. 1C). The PsbO2 band was not significantly different ($P = 0.49$) in plants with reduced total PsbO content. Given that these gels were loaded on a chlorophyll basis, this indicates that the PsbO2 change was in proportion to leaf chlorophyll content and thus also decreased on a per area basis (see below). Semiquantitative PCR using primers specific for *psbO1* and *psbO2* indicated that there was repression of mRNA for both isoforms relative to an 18S control in the lowest PsbO plants (Supplementary Fig. S1).

The two T2 lines with the greatest reductions in PsbO content, lines 8 and 15, exhibited a low $F_V/F_M$ phenotype (Fig. 2A) and small size (Fig. 3A, B). The low $F_V/F_M$ phenotype in these lines was related to both a decrease in $F_M$ and an increase in $F_O$, and was not explainable by PSI signal interference or dark acclimation time (data not shown). Other lines showing moderate reductions in PsbO content (lines 5, 7, and 16) exhibited no obvious $F_V/F_M$ phenotype. This biphasic response of $F_V/F_M$ was also evident when plotted against functional PSII (Fig. 2B). Chlorophyll fluorescence imaging demonstrated that this phenotype was consistent within a leaf and between leaves of different ages, indicating that the

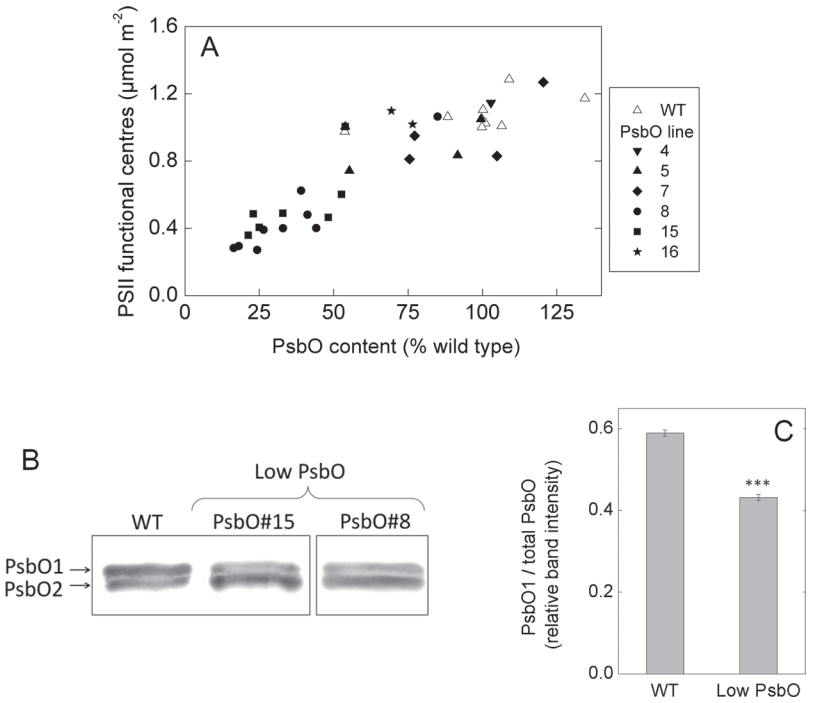


**Fig. 1.** (A) Relationship between total leaf PsbO protein content and functional (oxygen-evolving) PSII centres for a number of independent T2 antisense PsbO lines ($r^2$ = 0.79, $P$ < 0.0001). PsbO protein content was determined on a leaf area basis through Western blotting relative to a dilution series of a WT standard extraction. Functional PSII was determined from oxygen yield per single turnover flash (see Materials and Methods). (B) Resolution of the two PsbO isoforms from isolated thylakoids of a WT and two low PsbO transgenic lines. Gels were loaded on a chlorophyll basis (note from Table 1 that the chlorophyll content per leaf area in low PsbO plants is around half that of WT). The PsbO line 8 sample was run on the same gel but not on the adjacent lane. (C) The proportion of the total PsbO band intensity accounted for by the PsbO1 isoform. Shown are the averages and standard errors for three biological replicates of WT (mean PSII content 1.11 μmol $m^{-2}$) and low PsbO (lines #8 and #15, mean PSII content 0.47 μmol $m^{-2}$). ***, significant difference ($P$ = 0.0001).

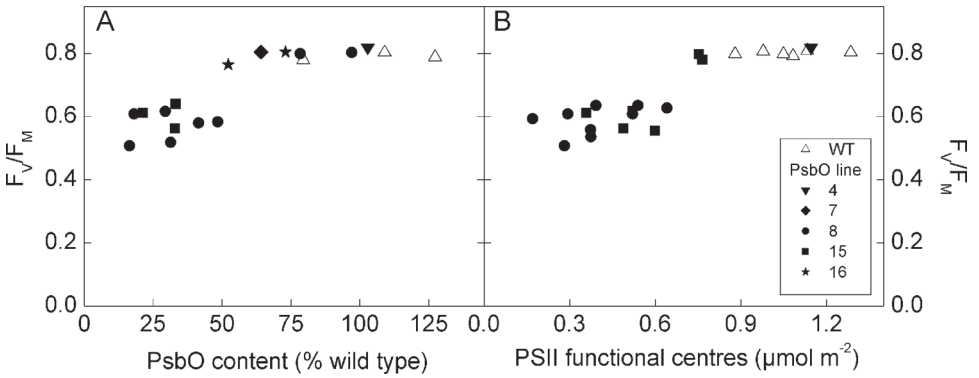


**Fig. 2.** Changes in the dark adapted maximum quantum yield from chlorophyll fluorescence ($F_V/F_M$) on the basis of PsbO protein content determined by Western blot (A) and on the basis of functional PSII content determined by the oxygen yield from single turnover flashes (B). The two data sets partially overlap but not all plants that had PsbO content measured were subsequently measured for functional PSII centres, and vice versa.

antisense effects was ontogenetically stable (Supplementary Fig. S2). Plants exhibiting an $F_V/F_M$ phenotype and less than 0.7 μmol $m^{-2}$ functional PSII centres (corresponding to approximately 50% PsbO) were designated as 'low PsbO' plants.

Given low PsbO plants appeared smaller at maturity than WT (Fig. 3A, B), growth rate was estimated by using the top view of the photosynthetic area as a non-destructive approximation for total leaf area (Table 1). Under the growth conditions used, low PsbO plants were slightly smaller than WT plants at the beginning of area measurements, and this difference was exacerbated over the 12 days of measurement such that relative rate of rosette area increase calculated from the top view of photosynthetic area

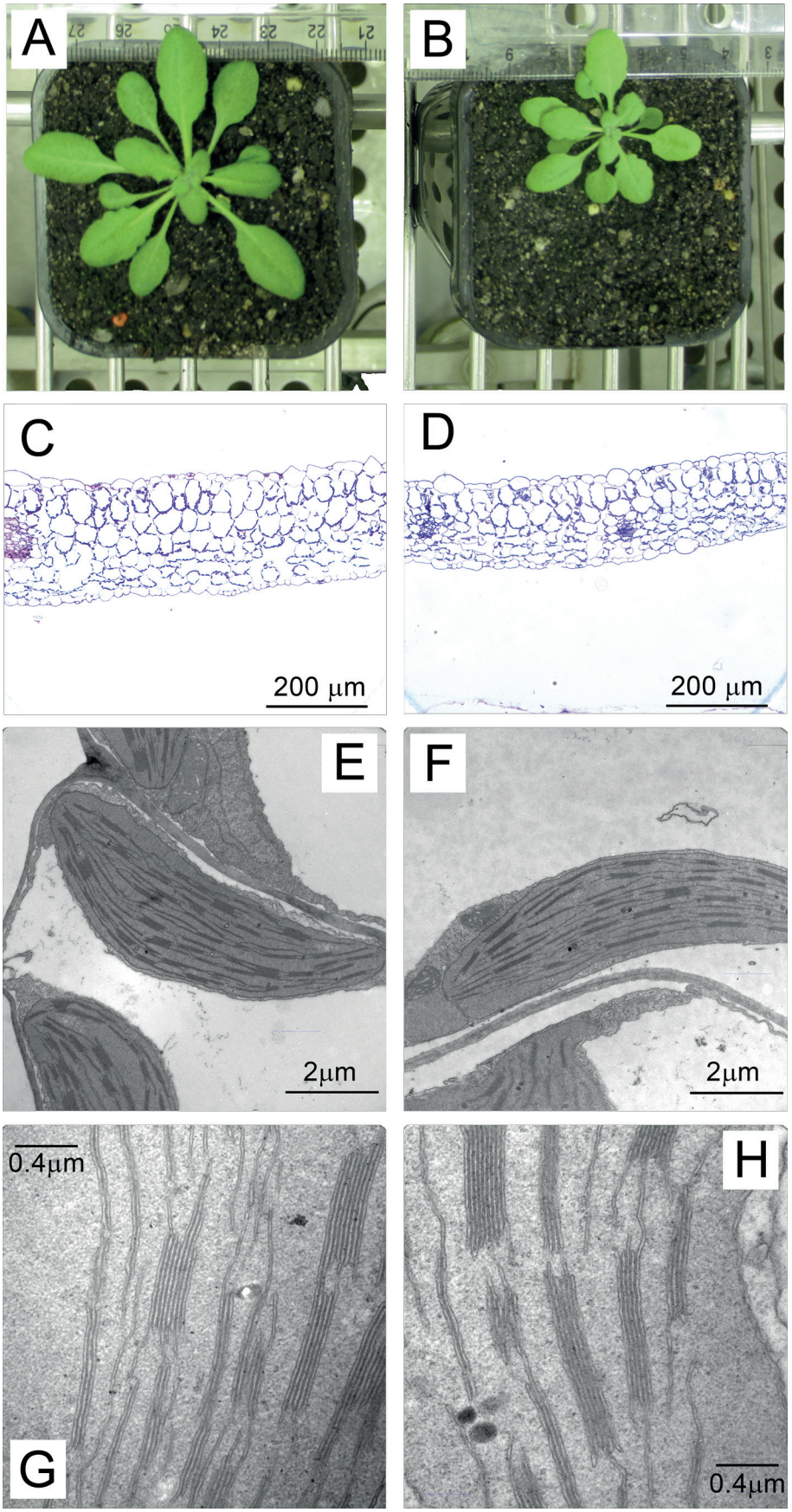


**Fig. 3.** Examples of phenotypic differences between WT (A, C, E, G) and low PsbO (B, D, F, H) plants: (A, B) growth differences, (C, D) transverse leaf sections (magnification ×200), (E–H) chloroplasts from palisade cells. Refer to Table 1 for quantifications from microscopy images. Bars, 200 μm (C, D), 2 μm (E, F), 0.4 μm (G, H) (this figure is available in colour at *JXB* online).

**Table 1.** Growth parameters and leaf characteristics of wild-type and low PsbO plants

Wild-type plants all have greater than 0.9 μmol $m^{-2}$ functional PSII centres and plants with low PsbO have less than 0.6 μmol $m^{-2}$ functional PSII centres. Average relative growth rate (RGR) over the course of the growth experiment was calculated by fitting an exponential to the data points of each individual plant. Initial surface area refers to that at the start of growth measurements (10 days after transfer from sucrose-supplemented growth media to soil) and final surface area that after a further 12 days (i.e. 22 days after transfer to soil). LMA, Leaf mass per area; $\triangle A$, absorbance proportional to P700 content, assuming the 810 nm measuring beam path length is constant between samples; Adaxial absorptance, absorptance to the xenon projector lamp used as the actinic source for light response measurements.

| | Wild type | | Low PsbO | | |
|---|---|---|---|---|---|
| | Mean ± SE | *n* | Mean ± SE | *n* | *P* |
| Relative rate of rosette area increase ($m^2$ $m^{-2}$ $day^{-1}$) | 0.19±0.00 | 5 | 0.13±0.01 | 7 | <0.0001 |
| Initial surface area ($cm^2$) | 3.29±0.16 | 5 | 2.08±0.38 | 7 | 0.0037 |
| Final surface area ($cm^2$) | 30.81±0.84 | 5 | 9.34±2.55 | 7 | <0.0001 |
| LMA dry (g $m^{-2}$) | 16.9±1.2 | 5 | 13.4±0.4 | 6 | 0.0130 |
| LMA fresh (g $m^{-2}$) | 258±18 | 5 | 196±9 | 6 | 0.0101 |
| Leaf dry mass/fresh mass | 0.066±0.001 | 5 | 0.070±0.003 | 6 | 0.1893 |
| Leaf thickness of fixed sections (μm) | 214±19 | 3 | 154±10 | 3 | 0.04808 |
| Leaf transverse cell layers | 8.42±0.22 | 3 | 7.50±0.52 | 3 | 0.1802 |
| Grana per chloroplast | 34.5±2.0 | 3 | 28.8±0.7 | 3 | 0.0562 |
| Thylakoid layers per grana | 4.87±0.14 | 3 | 5.66±0.17 | 3 | 0.0236 |
| Chl a (μmol $m^{-2}$) | 309±9 | 9 | 156±8 | 8 | <0.0001 |
| Chl b (μmol $m^{-2}$) | 79±2 | 9 | 51±3 | 8 | <0.0001 |
| Chl a/b | 3.9±0.1 | 9 | 3.1±0.1 | 8 | <0.0001 |
| $\Delta A_{max}$ (absorbance units × $10^3$) | 4.3±0.2 | 6 | 2.5±0.2 | 7 | 0.0001 |
| Adaxial absorptance | 0.76±0.01 | 7 | 0.73±0.01 | 9 | 0.0216 |

was reduced by one-third in these transgenics. Dry leaf mass per area was 21% lower in the low PsbO plants compared to WT, but leaf dry mass per fresh mass did not change.

Embedded leaf sections were 28% thinner in low PsbO plants compared to WT, though the number of transverse cell layers was not significantly different (Table 1 and Fig. 3C, D). Analysis of palisade chloroplasts showed that low PsbO mutants did not differ from WT in the number of grana stacks per chloroplast, but tended to have more thylakoid layers per granum (Table 1 and Fig. 3E–H).

### *Photosynthetic proteins*

The leaf content of proteins representing the major chloroplast electron transport complexes was quantified by Western blotting using the same WT standard extract used to quantify PsbO (Fig. 4). The core PSII subunit, PsbD (D2), decreased in parallel with PsbO content indicating the change in oxygen yield per single turnover flash was due to an absence of PSII centres (as opposed to assembled but non-functional centres). The PsaD protein of PSI also decreased, but only by approximately half this extent. A similar change was detected in maximum absorbance signal from $P700^+$, $\triangle A_{max}$. This parameter is proportional to photo-oxidizable P700 content and the change adds functional support to the finding of decreased PSI protein content (Table 1). While both PSII and PSI content was reduced on an area basis in low PsbO plants, the change in PSII was greater such that the ratio of PSII to PSI declined. No change was evident in the relative content per leaf area of the Rieske FeS protein of the cytochrome $b_6f$ complex or the AtpC subunit of ATP synthase. The assumption is made that only proteins formed into complexes are sufficiently stable to be measured by Western blot. Therefore, the absence of essential component proteins should reflect the absence of the complex. Rubisco catalytic sites per leaf area were determined separately, via the binding of the radioactively labelled

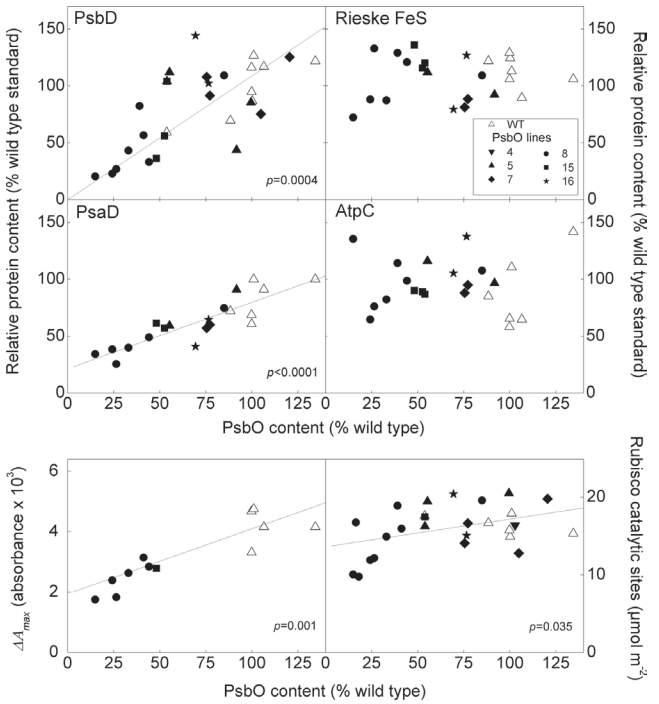


**Fig. 4.** Relationship between PsbO leaf protein content and major proteins representing the key steps in photosynthesis. PsbD (PSII), PsaD (PSI), Rieske FeS (cytochrome $b_6f$), and AtpC (ATP synthase) were determined by Western blotting. Total Rubisco catalytic sites was determined on a different set of plants by $^{14}$C-CABP binding. The $\Delta A_{max}$ parameter is proportional to total photo-oxidizable P700 content per area. It is included to give physiological support to the change in PSI content indicated by PsaD. Solid lines indicate a statistically significant relationship: for PsbD the regression equation is $y = 1.01x$; for PsaD, $y = 0.58 + 21.28$; for $\Delta A_{max}$, $y = 0.02x + 1.94$; for Rubisco, $y = 0.04x + 13.64$. Note that the slope of the regression line for PsaD is approximately half of that for PsbD.

inhibitor, [$^{14}$C]CABP. There was no change in Rubisco content in transgenic plants until PsbO content was reduced below 40%. Contents per unit leaf area of chlorophyll *a* and *b* were significantly less in the low PsbO plants, as was the chlorophyll *a*/*b* ratio (Table 1).

Cytochrome *f* content determined spectrophotometrically for a pooled leaf extract from four WT plants was 0.47±0.07 µmol $m^{-2}$. Given the lack of relationship between PsbO and Rieske FeS protein content, this value of cytochrome *f* was assumed to be consistent across the range of transgenics.

Blue native PAGE was performed to separate and visualize thylakoid membrane bound complexes in the native state. No major band shifts or missing/novel bands were evident in the low PsbO plants compared to the WT (Fig. 5). There was, however, an increase in the relative amount of LHCII not associated with a photosystem core. The sum of bands labelled LHCII assembly and LHCII trimer relative to the sum of all labelled bands for PsbO plants increased by 35% relative to WT. There was also a reduction in the sum of the PSII-LCHII supercomplexes compared to WT.

### *Photosynthetic physiology*

The gross oxygen evolution rate in response to increasing irradiance was measured on leaf pieces with an oxygen electrode under saturating $CO_2$ concentrations (Fig. 6). The quantum yield for oxygen evolution (the slope of the initial phase) decreased as PsbO content decreased, such that low PsbO plants exhibited a quantum yield 50% lower than the WT value of 0.10 oxygen per quantum (Fig. 7A). Maximum rates of oxygen evolution measured under saturating irradiances were independent of PsbO content, with a mean rate of 18.0±0.8 µmol $O_2$ $m^{-2}$ $s^{-1}$ (Fig. 7B). The combination of these characteristics meant that WT plants were light saturated at approximately 400 µmol quanta $m^{-2}$ $s^{-1}$, whereas low PsbO plants required between 600 and 800 µmol quanta $m^{-2}$ $s^{-1}$ to reach their maximum oxygen evolution rates.

Given that there was no change in the maximum oxygen evolution rate per leaf area (under saturated light and $CO_2$ conditions), the maximum oxygen evolution rate per total functional PSII increased in the low PsbO transgenics (Fig. 8). By plotting this parameter as a function of cytochrome $b_6f$ to PSII ratio, a hyperbolic relationship was obtained which was consistent with data recalculated from previous studies on pea and spinach (Evans, 1987b; Evans and Terashima, 1987; Terashima and Evans, 1988; Yamori *et al.*, 2008).

Chlorophyll *a* fluorescence was measured concurrently with oxygen evolution rates. Consistent with measured oxygen evolution rates, the PSII photochemical efficiency measured from chlorophyll fluorescence ($\Phi_{PSII}$, Genty *et al.*, 1989) was lower in low PsbO plants compared to WT at low irradiance (at approximately 80 µmol quanta $m^{-2}$ $s^{-1}$, $P < 0.0001$), but at saturating irradiances no differences were evident (at approximately 1050 µmol quanta $m^{-2}$ $s^{-1}$, $P = 0.29$; Fig. 9A). The quantum yield of non-photochemical quenching ($\Phi_{NPQ}$, Hendrickson *et al.*, 2004) was slightly higher in the low PsbO relative to WT plants at irradiances below 400 µmol quanta $m^{-2}$ $s^{-1}$, but slightly lower than WT at higher irradiances (Fig. 9B). The quantum yield of fluorescence and constitutive thermal energy dissipation, $\Phi_{f,D}$, was markedly higher in the low PsbO plants at all light intensities (Fig. 9C). While $\Phi_{f,D}$ increased with irradiance in the WT, in the transgenic plants it showed a decrease at light intensities above about 150 µmol quanta $m^{-2}$ $s^{-1}$. The fraction of 'open' PSII centres, $q_L$ (according to the shared antenna model of PSII, Kramer *et al.*, 2004b), declined faster in the WT plants as irradiance was increased and was lower compared to low PsbO plants at saturating irradiances ($P < 0.0001$; Fig. 9D). An estimated PSII

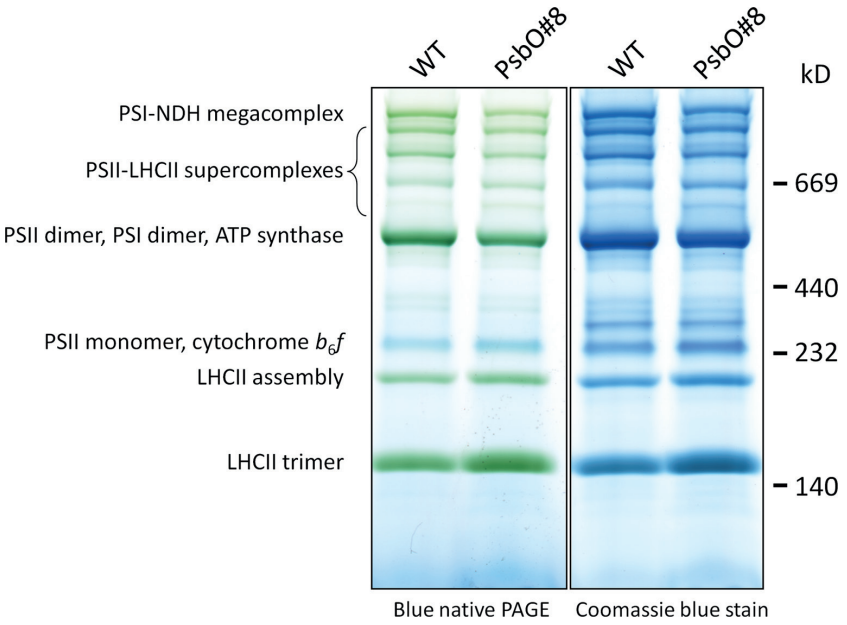


**Fig. 5.** Blue native polyacrylamide gel electrophoresis of isolated thylakoid membranes from a WT and a low PsbO plant. Gels were loaded on an equivalent chlorophyll basis (4 µg). The image shows the original Blue native gel and the same gel after further staining with Coomassie blue. Molecular weights are indicated with a High Molecular Weight Calibration Kit for native electrophoresis (GE Healthcare). Band identifications are taken from Järvi *et al.* (2011) (this figure is available in colour at *JXB* online).

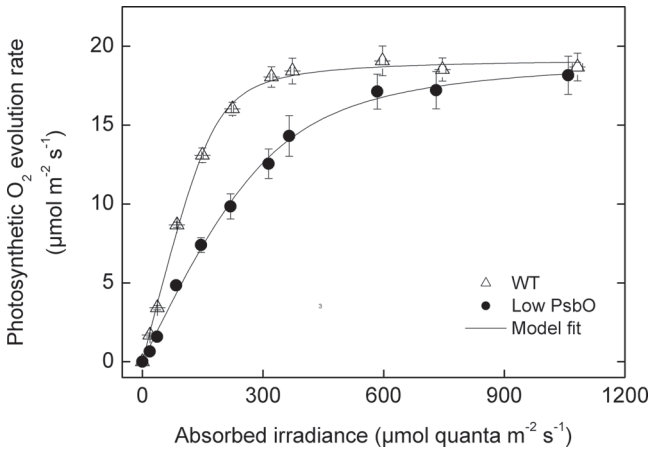


**Fig. 6.** Gross oxygen evolution per leaf area measured at approximately 1000 μbar $CO_2$ for WT plants (>0.85 μmol $m^{-2}$ functional PSII centres, $n$ = 5) and antisense mutants with low PSII functional centres (<0.6 μmol $m^{-2}$, $n$ = 8) PSII functional centres. Gross oxygen evolution rates were calculated relative to the signal drift in the dark, which was taken to be mitochondrial respiration. Solid lines are a fit of the average points to the model given in Equation 1. Model parameters for WT plants are $E_{Omax}$ = 19.25, θ = 0.93, $\Phi_O$ = 0.40. For low PsbO plants, $E_{Omax}$ =19.56, θ = 0.85, $\Phi_O$ = 0.21.

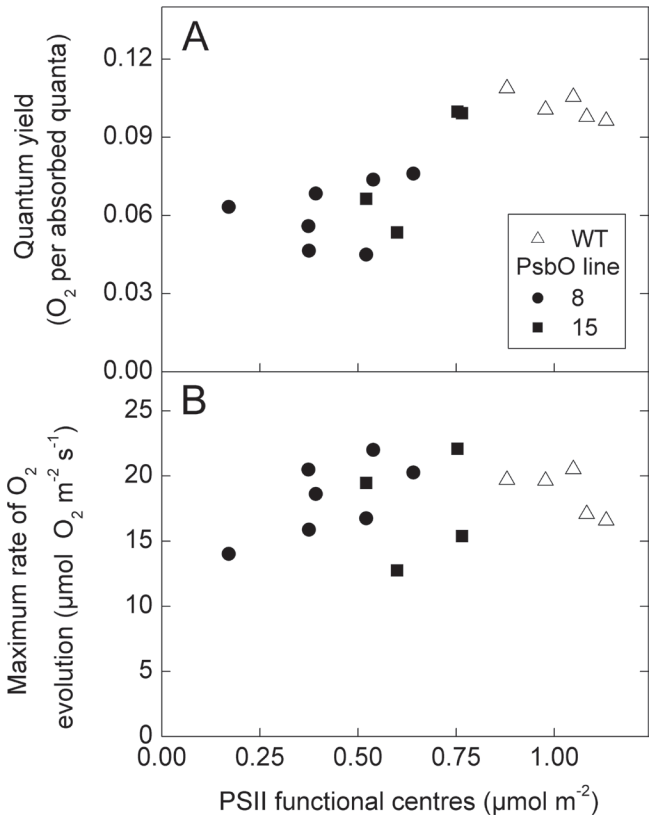


**Fig. 7.** Parameters from light response curves as a function of PSII functional centres. (A) The quantum yield for oxygen evolution, determined from the initial slope of light response curves. (B) The maximum rate of gross oxygen evolution, averaged from the three highest irradiances. There is a significant correlation between PSII functional centres and quantum yield ($r^2$ = 0.67, $P$ = 0.0001).

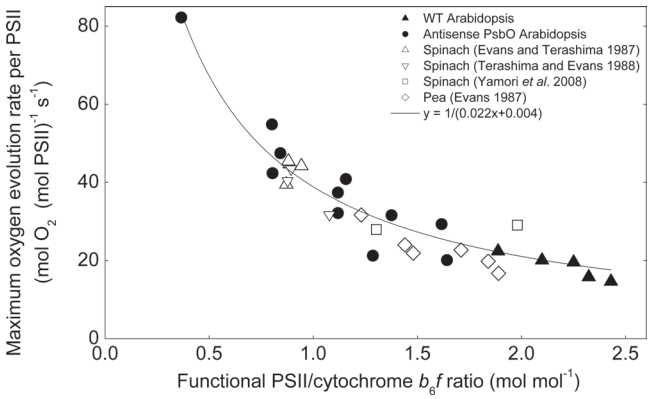


**Fig. 8.** Maximum oxygen evolution rates per leaf PSII content as a function of the PSII to cytochrome $b_6f$ ratio, for *Arabidopsis*, spinach, and pea. Open symbols are values calculated from other studies which have measured maximum electron transport-limited photosynthetic rate at 25 °C, total PSII centres and cytochrome $b_6f$ content: spinach grown under various nitrogen nutrition (Evans and Terashima, 1987), irradiance (Terashima and Evans, 1988), and temperature (Yamori *et al.*, 2008); and pea grown under various irradiance (Evans, 1987b). For atrazine binding, measurements were converted to the equivalent functional PSII measurements obtained through flash yield, by dividing by 1.14 (Chow and Anderson, 1987; Chow *et al.*, 1989). For Yamori *et al.* (2008) PSII centres were estimated from the chlorophyll content and cytochrome *f* content taken from Yamori *et al.* (2005). The line is a fit to the *Arabidopsis* data only ($r^2$ = 0.93).

to PSI light partitioning factor, X (Equation 3), can be obtained by combining fluorescence parameters with oxygen evolution rates (Fig. 9E). Wild-type plants varied around 0.5 at all irradiances, whereas low PsbO plants varied from 0.4 at irradiances below 50 μmol quanta $m^{-2}$ $s^{-1}$ to 0.5 between 50 and 350 μmol quanta $m^{-2}$ $s^{-1}$, before increasing to 0.6 at irradiances greater than 400 μmol quanta $m^{-2}$ $s^{-1}$. Measurements of chlorophyll fluorescence and photosynthetic $O_2$ evolution gave qualitatively similar responses for photosynthetic electron transport to irradiance.

## Discussion

### *Reduction in PsbO content leads to reduced PSII content and low quantum yield*

The aim of this study was to gain a better understanding of the rate-limiting potential of photosystem II (PSII) in photosynthesis *in vivo* by creating transgenic *A. thaliana* plants with reductions in the total amount of PsbO proteins. Plants with 25–60% of wild-type PsbO protein levels were produced. Both PsbO isoforms were decreased on a leaf area basis, but the antisense had a greater effect on the more abundant PsbO1 isoform. PsbO2 was reduced to a lesser extent, in approximate proportion to reductions in chlorophyll content, and thus the PsbO1/PsbO2 ratio was altered in these plants (Fig. 1). Previous studies of *A. thaliana* mutants have shown that in the absence of one PsbO isoform, the other isoform tends to accumulate in compensation (Murakami *et al.*, 2002, 2005; Lundin *et al.*, 2007). Given that total PsbO

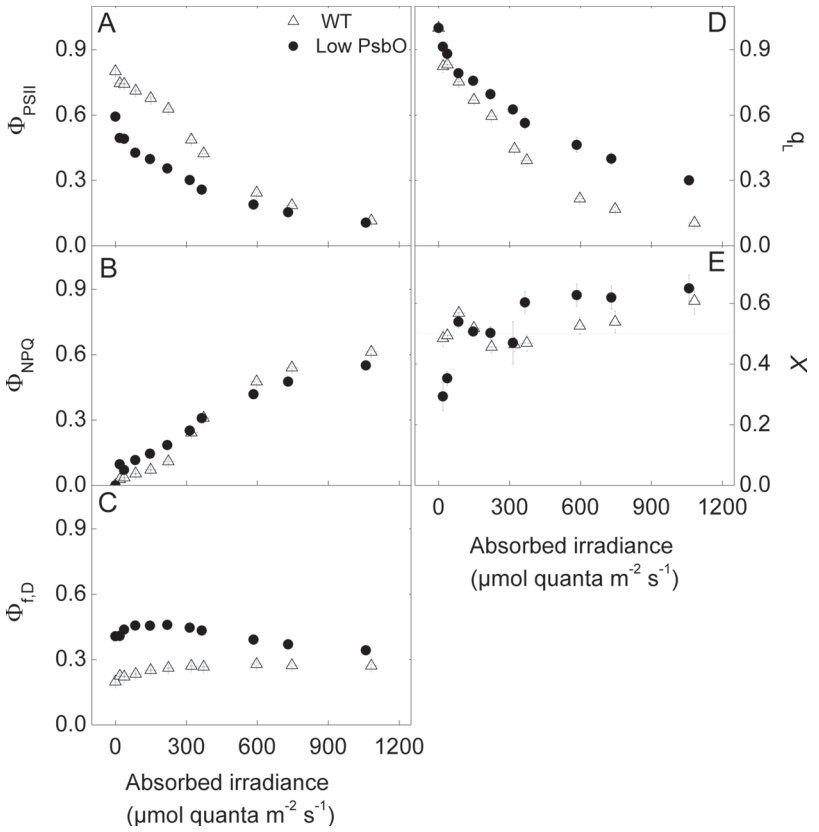


**Fig. 9.** Fluorescence parameters measured concurrently with oxygen evolution rates. (A) The quantum yield of PSII, $\Phi_{PSII}$, given by $\frac{(F_M' - F_s)}{F_M'}$ (Genty et al., 1989). (B′) The quantum yield of non-photochemical quenching, $\Phi_{NPQ}$, given by $\left(\frac{F_s}{F_M'} - \frac{F_s}{F_M}\right)$ (Hendrickson et al., 2004). (C) The quantum yield of fluorescence and constitutive thermal energy dissipation, $\Phi_{f,D}$, given by $\frac{F_s}{F_M}$ (Hendrickson et al., 2004). (D) The proportion of 'open' PSII centres, $q_L$, given by $\frac{F_M' - F_s}{F_M' - F_0'} \bullet \frac{F_0'}{F_s}$ (Kramer et al., 2004b), where F'$_O$ was calculated according to Oxborough and Baker (1997b). (E) An estimation of the proportion of absorbed irradiance used for water splitting at PSII, *X*, calculated according to Equation 3. The dashed line at 0.5 shows the expected value if PSII and PSI centres were using an equal proportion of the absorbed light.

content in the antisense mutants was decreased to such a degree and with no hyper-accumulation of PsbO2 on either a chlorophyll or leaf area basis, it may be concluded that the antisense construct led to a decrease in expression of both PsbO isoforms (see also gene expression data in Supplementary Fig. S1).

Reductions to oxygen evolving (functional) PSII centres were almost directly proportional to reductions in total PsbO. Low PsbO mutants had less than a third of the wild-type content of PSII centres per unit leaf area. The amount of D2 protein of the PSII core was also reduced almost one to one with PsbO content (Fig. 4). The D2 protein is the first building block for PSII assembly and is stable relative to the rapidly turned over D1 protein (Minai *et al.*, 2006). Therefore the decrease in D2 amount indicates that the decrease in oxygen yield per single turnover flash was due to a simple absence of PSII centres, and there was not an accumulation of assembled (or partly assembled) but non-functional PSII centres in the leaf. Blue native PAGE is consistent with this conclusion, as there were no band shifts or additional bands that might suggest the presence of unusually assembled PSII centres (Fig. 5).

The quantum yield of PSII gives a measure of the efficiency of the conversion of excitation energy into electron transport. Here the quantum yield was measured in two ways: through PSII photochemical efficiency calculated from chlorophyll fluorescence and from the initial slope of a light response curve of oxygen evolution, $\Phi_O$ (Figs. 2 and 6 and Equation 1). The reduction in quantum yield indicates a decrease in the functional efficiency of the PSII centres present in the leaves of low PsbO plants. This phenotype has been noted in plants with reduced PsbO1, but not in plants with reduced PsbO2 (Murakami *et al.*, 2002, 2005; Lundin *et al.*, 2007), and here is also correlated with a decrease in PsbO1/PsbO2 ratio, as demonstrated in Fig. 1. As growth irradiance (200 µmol quanta m$^{-2}$ s$^{-1}$) falls within the light limited region of the irradiance response curves for both WT and low PsbO plants (Fig. 6), the difference in quantum yields would contribute to the 32% reduction in rosette expansion in low PsbO plants (Table 1).

### *Low PsbO plants have lower chlorophyll a/b ratios and reduced PSI content*

One of the strengths of antisense techniques is that the protein or component of interest can often be targeted with minimal effects in other components and that a range of reductions in the target

component can be achieved. Manipulating the stoichiometry of photosynthetic components in this way provide information as to how the complexes interact, colimit, and regulate (Furbank and Taylor, 1995; Raines, 2003). Despite the perturbation to PSII which is conceptually the first enzymatic step in photosynthesis, low PsbO plants did not exhibit changes in the quantity of Rubisco or proteins representing ATP synthase and cytochrome $b_6f$ (Fig. 4). The lack of change detected in cytochrome $b_6f$ content is important given its position between PSII and PSI, its role as one of the important limiting steps to electron transport rate and that cytochrome $b_6f$ content is highly regulated by growth irradiance (Anderson, 1992; Anderson *et al.*, 1988; Evans, 1987b; Yamori *et al.*, 2011b).

There were some significant pleiotropic changes in the photosynthetic biochemistry of low PsbO plants, however. Notably, a decrease in chlorophyll content, a decrease in the chlorophyll *a/b* ratio (Table 1) and a decrease in PSI content (Fig. 4). The reduction in PSI content was approximately half the extent of the reduction in PSII, and was in proportion to the overall decrease in chlorophyll content. Physiological measurements of P700, the primary electron donor of PSI, although less marked, give qualitative support to this protein-based conclusion (Fig. 4). The quantitation of PSI from P700 absorbance is complicated by signal contamination from plastocyanin. This contamination was controlled with the dual-wavelength approach used here (see Methods), but could be further eliminated by using a three-wavelength approach (Kirchhoff *et al.*, 2004). Photosystem II to PSI ratio is an important factor in determining photosynthetic efficiency (Kramer and Evans, 2011) and leaves grown under light conditions that preferentially excites one or the other photosystem will adjust the stoichiometry of the two in order to maintain an effective linear electron transport and quantum yield under growth conditions (Chow *et al.*, 1990). The redox state of plastoquinone (PQ), the lipid-soluble electron carrier between PSII and cytochrome $b_6f$, appears to be a key regulatory signal for this adjustment PSII to PSI ratio (Pfannschmidt *et al.*, 1999; Allen and Pfannschmidt, 2000; Shimizu *et al.*, 2010). It is intriguing in this case that PSI content was decreased while cytochrome $b_6f$ remained unchanged.

Decreases in chlorophyll *a/b* ratio are generally driven by increased expression in the chlorophyll *b*-rich peripheral light harvesting complexes (LHC) per photosystem as an adaptive response to low light, increasing energy capture (Anderson *et al.*, 1988; Bailey *et al.*, 2001) for a minimal protein investment (Evans, 1987b). While reductions in PSII and PSI content would lower the chlorophyll *a/b* ratio (as the core pigments are mostly chlorophyll *a*), there may be additional changes to LHC expression driven by factors such as an altered redox state of the PQ pool. There was a reduction in LHC content per unit leaf area in the low PsbO plants, but LHC increased on a chlorophyll basis, as evidenced by the lower chlorophyll *a/b* ratio and increase in LHC complexes in the Blue native gel (Fig. 5). The reduction in quantum yield and high $F_O$ and $\Phi_{f,D}$ in the low PsbO plants suggest a decrease in the effectiveness of energy transfer from LHCs to PSII.

Increased chlorophyll *a/b* ratios, have also been noted in antisense plants with reduced ferredoxin content that leads to increased PQ reduction (Holtgrefe *et al.*, 2003). In contrast, this effect was not apparent in tobacco plants with reductions in the Rieske FeS protein of cytochrome $b_6f$, despite a highly reduced PQ pool, with the authors speculating that an interaction between the PQ redox state and the missing cytochrome $b_6f$ complex is required for regulation of peripheral light harvesting complexes (Anderson *et al.*, 1997). In the case of low PsbO plants, cytochrome $b_6f$ content remained unchanged.

### *PSII capacity is not limiting to light-saturated electron transport rate*

The oxygen evolution rate per total leaf PSII centres was calculated by dividing the light- and $CO_2$-saturated photosynthetic rates by the PSII functional centres determined by the single turnover flash method (Fig. 8). This gives a 'PSII-normalized' chloroplast electron transport rate under light-saturated conditions. Altering the amount of functional PSII centres by antisense techniques produced a wide variation in this parameter in *A. thaliana*, from just 18 mol $O_2$ (mol PSII)$^{-1}$ s$^{-1}$ in WT plants to over 50 mol $O_2$ (mol PSII)$^{-1}$ s$^{-1}$ in the low PsbO transgenics. As functional PSII decreased to minimal values, there was no apparent plateau in PSII-normalized electron transport rate (Fig. 8), nor a decrease in maximum photosynthetic rate (Fig. 7). Low PsbO plants appear to maintain a greater proportion of 'open' PSII centres at high light, as determined by the chlorophyll fluorescence parameter, $q_L$ (Fig. 9D).

There was a hyperbolic relationship between oxygen evolution rate per PSII centre and PSII per unit cytochrome $b_6f$ in *A. thaliana* (Fig. 8). This parameter was calculated (at 25 °C) for pea and spinach from previous studies where the leaf PSII to cytochrome $b_6f$ ratio varied in response to light, nutrient, and growth temperature treatments (Evans, 1987b; Evans and Terashima, 1987; Terashima and Evans, 1988; Yamori *et al.*, 2008). These species share the same hyperbolic relationship which can be written as $P_{max}/p = 1/(0.022 \times p/f + 0.004)$, where $P_{max}$ is the maximum oxygen evolution rate, $p$ is the PSII content, and $f$ the cytochrome $b_6f$ content (from the regression line in Fig. 8). Rearrangement of the above equation gives:

$$P_{max} = \frac{1}{\frac{0.022}{f} + \frac{0.004}{p}}$$

It is seen that $P_{max}$ decreases when either $f$ or $p$ decreases. However, since $p$ is approximately twice as large as $f$ in WT *Arabidopsis*, the first term in the denominator is more than 10-fold larger than the second term. This finding is consistent with cytochrome $b_6f$, rather than PSII, being the most rate-limiting step to light-saturated chloroplast electron transport rates under moderate temperature conditions and therefore being a bottleneck in the light-saturated flow of electrons from PSII to PSI (Evans, 1988; Makino *et al.*, 1994; Price *et al.*, 1995, 1998; Yamori *et al.*, 2010, 2011b). At high light, electron transport from PSII is modulated by changing $q_L$ to match the maximum electron transport rate allowed by the amount of cytochrome $b_6f$.

This degree of insensitivity of maximum photosynthetic rate to PSII functional amount has been termed the 'excess capacity'

of PSII (Behrenfeld *et al.*, 1998; Kaňa *et al.*, 2002) relative to cytochrome $b_6f$ at saturating light intensities. This study demonstrates this without the requirement for photoinhibitory treatments or herbicides to manipulate PSII functional centres.

Light-saturated PSII capacity has previously been studied using combinations of photoinhibition and herbicides to manipulate the number of active PSII centres in a leaf (Behrenfeld *et al.*, 1998; Lee *et al.*, 1999; Kaňa *et al.*, 2002). These studies found that PSII became rate limiting to maximum (light-saturated) photosynthetic rate with 40% (in detached capsicum leaves, Lee *et al.*, 1999) to 50% (in phytoplankton assemblages, Behrenfeld *et al.*, 1998; in green algae, Kaňa *et al.*, 2002) deactivation. In this study PSII functional amount was decreased by 75% without a measurable decrease in light- and $CO_2$-saturated photosynthetic rate. Using the results from capsicum leaves in Lee *et al.* (1999), the maximum oxygen evolution rate per remaining active PSII centre reaches before it becomes limiting is approximately 25 mol $O_2$ (mol PSII)$^{-1}$ s$^{-1}$, lower than this parameter achieved in low PsbO *A. thaliana* and lower than for spinach and pea measured under non-photoinhibitory conditions (Fig. 8, data calculated from Evans, 1987b; Evans and Terashima, 1987; Terashima and Evans, 1988; Yamori *et al.*, 2008). A key difference between these approaches and the antisense approach used here is that low PsbO plants simply lack PSII centres, whereas under photoinhibitory conditions it is likely that inactivated PSII centres accumulate in the thylakoid membrane. Kirchhoff *et al.* (2000) have demonstrated that diffusion of PQ can become a limiting factor to chloroplast electron transport rate due to the formation of microdomains in the thylakoid membrane preventing the free diffusion of reduced PQ from PSII to cytochrome $b_6f$. Therefore it is possible that photosynthesis after photoinhibition of PSII is not limited by the capacity of PSII itself, but by the PQ diffusion limitations in the thylakoid membrane caused by macromolecular crowding from inactive (non-reducing) PSII centres. The lack of inactivated PSII centres in the low PsbO plants allows PQ diffusion to proceed at normal levels, thus leaving chloroplast electron transport limited by cytochrome $b_6f$.

## Conclusions

The most notable changes in the low PsbO plants were a decrease in the number of PSII centres per unit leaf area and lowered efficiency of those PSII centres that remained. This reduced quantum yield under low irradiance, but maximum light-saturated photosynthetic rates were unchanged despite having fewer PSII centres per unit leaf area. The reduction in quantum yield is a likely explanation for the reduced growth rate of low PsbO plants. A decrease in the number of PSII centres is not expected to lower quantum yield *per se*, so long as they are functional and the distribution of excitation energy between PSII and PSI is balanced (Kramer and Evans, 2011). There was more chlorophyll and LHCII content per PSII in low PsbO leaves, but it is not known how the different pigment protein complexes function together as effective antennae to PSII. The observed decrease in PSII efficiency may be due to impaired transfer of excitation energy from the light harvesting pigments to the PSII reaction centre in low PsbO plants associated with the increase in chlorophyll and LHCII content per PSII.

## Supplementary material

Supplementary data are available at *JXB* online.

Supplementary methods. Conversion of a P700 transmittance signal to absorbance units

Supplementary Fig. S1. Semiquantitative PCR on *PsbO1* and *PsbO2* expression

Supplementary Fig. S2. Chlorophyll fluorescence images of an antisense plant with low PsbO content and a WT plant, demonstrating the consistency of $F_V/F_M$ changes within and between leaves.

## Acknowledgements

This work was supported by an Australian Postgraduate Award to SAD, the Australian Research Council Centre of Excellence in Plant Energy Biology (MRB), and grants from the Australian Research Council (WSC). For technical assistance and advice on methods the authors thank Benedict Long, Jasper Pengelly, Soumi Bala, and Husen Jia from the Research School of Biology, ANU. Cathy Gillespie of the John Curtin School of Medical Research, ANU, sectioned, stained and imaged for TEM.

## References

**AllahverdiyevaY, Mamedov F, Holmstrom M, Nurmi M, Lundin B, Styring S, Spetea C, Aro EM.** 2009. Comparison of the electron transport properties of the *psbo1* and *psbo2* mutants of *Arabidopsis thaliana*. *Biochimica et Biophysica Acta – Bioenergetics* **1787,** 1230–1237.

**Allen JF, Pfannschmidt T.** 2000. Balancing the two photosystems: photosynthetic electron transfer governs transcription of reaction centre genes in chloroplasts. *Philosophical Transactions of the Royal Society of London. Series B: Biological Sciences* **355,** 1351–1359.

**Altschul SF, Madden TL, Schäffer AA, Zhang J, Zhang Z, Miller W, Lipman DJ.** 1997. Gapped BLAST and PSI-BLAST: a new generation of protein database search programs. *Nucleic Acids Research* **25,** 3389–3402.

**Anderson JM.** 1992. Cytochrome $b_6f$ complex: *dynamic molecular organization*, function and acclimation. *Photosynthesis Research* **34,** 341–357.

**Anderson JM, Chow WS, Goodchild DJ.** 1988. Thylakoid membrane organisation in sun/shade acclimation. *Functional Plant Biology* **15,** 11–26.

**Anderson JM, Price GD, Chow WS, Hope AB, Badger MR.** 1997. Reduced levels of cytochrome *bf* complex in transgenic tobacco leads to marked photochemical reduction of the plastoquinone pool, without significant change in acclimation to irradiance. *Photosynthesis Research* **53,** 215–227.

**Andersson B, Barber J.** 1996. Mechanisms of photodamage and protein degradation during photoinhibition of photosystem II. In: NB Baker, editor, *Photosynthesis and the Environment*. Dordrecht. Kluwer Academic Publishers, pp 101–121.

**Andersson B, Salter AH, Virgin I, Vass I, Styring S.** 1992. Photodamage to photosystem II–primary and secondary events. *Journal of Photochemistry and Photobiology B: Biology* **15,** 15–31.

**Andersson J, Walters RG, Horton P, Jansson S.** 2001. Antisense inhibition of the photosynthetic antenna proteins CP29 and CP26:

implications for the mechanism of protective energy dissipation. *The Plant Cell* **13,** 1193–1204.

**Bailey S, Walters RG, Jansson S, Horton P.** 2001. Acclimation of *Arabidopsis thaliana* to the light environment: the existence of separate low light and high light responses. *Planta* **213,** 794–801.

**Barber J.** 2006. Photosystem II: an enzyme of global significance. *Biochemical Society Transactions* **34,** 619–631.

**Behrenfeld MJ, Prasil O, Kolber ZS, Babin M, Falkowski PG.** 1998. Compensatory changes in photosystem II electron turnover rates protect photosynthesis from photoinhibition. *Photosynthesis Research* **58,** 259–268.

**Bendall DS, Davenport HE, Hill R.** 1971. Cytochrome components in chloroplasts of the higher plants. *Methods: A Companion to Methods in Enzymology* **23,** 327–344.

**Berry J, Björkman O.** 1980. Photosynthetic response and adaptation to temperature in higher plants. *Annual Review of Plant Physiology* **31,** 491–543.

**Bricker TM.** 1992. Oxygen evolution in the absence of the 33-kilodalton manganese-stabilizing protein. *Biochemistry* **31,** 4623–4628.

**Bricker TM, Frankel LK.** 1998. The structure and function of the 33 kDa extrinsic protein of photosystem II: a critical assessment. *Photosynthesis Research* **56,** 157–173.

**Bricker TM, Frankel LK.** 2008. The *psbo1* mutant of *Arabidopsis* cannot efficiently use calcium in support of oxygen evolution by photosystem II. *Journal of Biological Chemistry* **283,** 29022–29027.

**Burnap RL, Sherman LA.** 1991. Deletion mutagenesis in *Synechocystis* sp. PCC6803 indicates that the Mn-stabilizing protein of photosystem II is not essential for $O_2$ evolution. *Biochemistry* **30,** 440–446.

**Chow WS, Anderson JM.** 1987. Photosynthetic responses of *Pisum sativum* to an increase in irradiance during growth. II. Thylakoid membrane components. *Functional Plant Biology* **14,** 9–19.

**Chow WS, Hope AB, Anderson JM.** 1989. Oxygen per flash from leaf disks quantifies photosystem II. *Biochimica et Biophysica Acta* **973,** 105–108.

**Chow WS, Hope AB, Anderson JM.** 1991. Further studies on quantifying photosystem II *in vivo* by flash-induced oxygen yield from leaf disks. *Australian Journal of Plant Physiology* **18,** 397–410.

**Chow WS, Melis A, Anderson JM.** 1990. Adjustments of photosystem stoichiometry in chloroplasts improve the quantum efficiency of photosynthesis. *Proceedings of the National Academy of Sciences, USA* **87,** 7502–7506.

**Clough SJ, Bent AF.** 1998. Floral dip: a simplified method for *Agrobacterium*-mediated transformation of *Arabidopsis thaliana*. *The Plant Journal* **16,** 735–743.

**Curtis MD, Grossniklaus U.** 2003. A gateway cloning vector set for high-throughput functional analysis of genes *in planta*. *Plant Physiology* **133,** 462–469.

**Dwyer SA, Ghannoum O, Nicotra AB, von Caemmerer S.** 2007. High temperature acclimation of $C_4$ photosynthesis is linked to changes in photosynthetic biochemistry. *Plant, Cell and Environment* **30,** 53–66.

**Evans JR.** 1987a. The dependence of quantum yield on wavelength and growth irradiance. *Australian Journal of Plant Physiology* **14,** 69–79.

**Evans JR.** 1987b. The relationship between electron transport components and photosynthetic capacity in pea leaves grown at different irradiances. *Australian Journal of Plant Physiology* **14,** 157–170.

**Evans JR.** 1988. Acclimation by the thylakoid membranes to growth irradiance and the partitioning of nitrogen between soluble and thylakoid proteins. *Functional Plant Biology* **15,** 93–106.

**Evans JR, Terashima I.** 1987. Effects of nitrogen nutrition on electron transport components and photosynthesis in spinach. *Australian Journal of Plant Physiology* **14,** 59–68.

**Farage PK, Long SP.** 1991. The occurrence of photoinhibition in an over-wintering crop of oil-seed rape (*Brassica napus* L.) and its correlation with changes in crop growth. *Planta* **185,** 279–286.

**Farquhar GD, von Caemmerer SV, Berry JA.** 1980. A biochemical model of photosynthetic $CO_2$ assimilation in leaves of $C_3$ species. *Planta* **149,** 78–90.

**Furbank RT, Taylor WC.** 1995. Regulation of photosynthesis in $C_3$ and $C_4$ plants: a molecular approach. *The Plant Cell* **7,** 797–807.

**García-Cerdán JG, Sveshnikov D, Dewez D, Jansson S, Funk C, Schröder WP.** 2009. Antisense inhibition of the PsbX protein affects PSII integrity in the higher plant *Arabidopsis thaliana*. *Plant and Cell Physiology* **50,** 191–202.

**Genty B, Briantais J, Baker NB.** 1989. The relationship between the quantum yield of photosynthetic eletron transport and quenching of chlorohyll fluorescence. *Biochimica et Biophysica Acta* **990,** 87–92.

**Greer DH, Berry JA, Björkman O.** 1986. Photoinhibition of photosynthesis in intact bean leaves: role of light and temperature, and requirement for chloroplast-protein synthesis during recovery. *Planta* **168,** 253–260.

**Haldrup A, Lunde C, Scheller HV.** 2003. *Arabidopsis thaliana* plants lacking the PSI-D subunit of photosystem I suffer severe photoinhibition, have unstable photosystem I complexes, and altered redox homeostasis in the chloroplast stroma. *Journal of Biological Chemistry* **278,** 33276–33283.

**Hendrickson L, Furbank RT, Chow WS.** 2004. A simple alternative approach to assessing the fate of absorbed light energy using chlorophyll fluorescence. *Photosynthesis Research* **82,** 73–81.

**Holtgrefe S, Bader KP, Horton P, Scheibe R, von Schaewen A, Backhausen JE.** 2003. Decreased content of leaf ferredoxin changes electron distribution and limits photosynthesis in transgenic potato plants. *Plant Physiology* **133,** 1768–1778.

**Huntzinger E, Izaurralde E.** 2011. Gene silencing by microRNAs: contributions of translational repression and mRNA decay. *Nature Reviews Genetics* **12,** 99–110.

**Järvi S, Suorsa M, Paakkarinen V, Aro EM.** 2011. Optimized native gel systems for separation of thylakoid protein complexes: novel super- and mega-complexes. *The Biochemical Journal* **439,** 207–214.

**Kaňa R, Lazár D, Prášil O, Nauš J.** 2002. Experimental and theoretical studies on the excess capacity of photosystem II. *Photosynthesis Research* **72,** 271–284.

**Kanazawa A, Kramer DM.** 2002. *In vivo* modulation of nonphotochemical exciton quenching (NPQ) by regulation of the chloroplast ATP synthase. *Proceedings of the National Academy of Sciences, USA* **99,** 12789–12794.

**Kirchhoff H, Horstmann S, Weis E.** 2000. Control of the photosynthetic electron transport by PQ diffusion microdomains in thylakoids of higher plants. *Biochimica et Biophysica Acta – Bioenergetics* **1459,** 148–168.

**Kirchhoff H, Schöttler MA, Maurer J, Weis E.** 2004. Plastocyanin redox kinetics in spinach chloroplasts: evidence for disequilibrium in the high potential chain. *Biochimica et Biophysica Acta – Bioenergetics* **1659,** 63–72.

**Kramer DM, Avenson TJ, Edwards GE.** 2004a. Dynamic flexibility in the light reactions of photosynthesis governed by both electron and proton transfer reactions. *Trends in Plant Science* **9,** 349–357.

**Kramer DM, Evans J.** 2011. Update: the importance of energy balance in improving photosynthetic productivity. *Plant Physiology* **155,** 70–78.

**Kramer DM, Johnson G, Kiirats O, Edwards GE.** 2004b. New fluorescence parameters for the determination of $Q_A$ redox state and excitation energy fluxes. *Photosynthesis Research* **79,** 209–218.

**Kuwabara T, Murata N.** 1983. Quantitative analysis of the inactivation of photosynthetic oxygen evolution and the release of polypeptides and manganese in the photosystem II particles of spinach chloroplasts. *Plant and Cell Physiology* **24,** 741–747.

**Lazo GR, Stein PA, Ludwig RA.** 1991. A DNA transformation-competent *Arabidopsis* genomic library in *Agrobacterium*. *Nature Biotechnology* **9,** 963–967.

**Lee H-Y, Chow WS, Hong Y-N.** 1999. Photoinactivation of photosystem II in leaves of *Capsicum annuum*. *Physiologia Plantarum* **105,** 376–383.

**Leuschner C, Bricker TM.** 1996. Interaction of the 33 kDa extrinsic protein with photosystem II: rebinding of the 33 kDa extrinsic protein to photosystem II membranes which contain four, two, or zero manganese per photosystem II reaction center. *Biochemistry* **35,** 4551–4557.

**Long SP, Farage PK, Aguilera C, Macharia JMN.** 1992. *Damage to photosynthesis during chilling and freezing, and its significance to the photosynthetic productivity of field crops*. In: J Barber, H Guerrero, H Mendrano, editors, *Trends in Photosynthesis Research*. Hampshire, UK. Intercept, pp 345–356.

**Long SP, Humphries S, Falkowski PG.** 1994. Photoinhibition of photosynthesis in nature. *Annual Review of Plant Physiology and Plant Molecular Biology* **45,** 633–662.

**Losciale P, Oguchi R, Hendrickson L, Hope AB, Corelli-Grappadelli L, Chow WS.** 2008. A rapid, whole-tissue determination of the functional fraction of PSII after photoinhibition of leaves based on flash-induced P700 redox kinetics. *Physiologia Plantarum* **132,** 23–32.

**Lundin B, Hansson M, Schoefs B, Vener AV, Spetea C.** 2007. The *Arabidopsis* PsbO2 protein regulates dephosphorylation and turnover of the photosystem II reaction centre D1 protein. *The Plant Journal* **49,** 528–539.

**Lundin B, Nurmi M, Rojas-Stuetz M, Aro E-M, Adamska I, Spetea C.** 2008. Towards understanding the functional difference between the two PsbO isoforms in *Arabidopsis thaliana* – insights from phenotypic analyses of *psbo* knockout mutants. *Photosynthesis Research* **98,** 405–414.

**Makino A, Nakano H, Mae T.** 1994. Effects of growth temperature on the responses of ribulose-1,5-biphosphate carboxylase, electron transport components, and sucrose synthesis enzymes to leaf nitrogen in rice, and their relationships to photosynthesis. *Plant Physiology* **105,** 1231–1238.

**Maxwell K, Johnson GN.** 2000. Chlorophyll fluorescence – a practical guide. *Journal of Experimental Botany* **51,** 659–668.

**Mayfield SP, Bennoun P, Rochaix JD.** 1987a. Expression of the nuclear encoded OEE1 protein is required for oxygen evolution and stability of photosystem II particles in *Chlamydomonas reinhardtii*. *The EMBO Journal* **6,** 313–318.

**Mayfield SP, Rahire M, Frank G, Zuber H, Rochaix JD.** 1987b. Expression of the nuclear gene encoding oxygen-evolving enhancer protein 2 is required for high-levels of photosynthetic oxygen evolution in *Chlamydomonas reinhardtii*. *Proceedings of the National Academy of Sciences, USA* **84,** 749–753.

**Minai L, Wostrikoff K, Wollman F-A, Choquet Y.** 2006. Chloroplast biogenesis of photosystem II cores involves a series of assembly-controlled steps that regulate translation. *The Plant Cell* **18,** 159–175.

**Murakami R, Ifuku K, Takabayashi A, Shikanai T, Endo T, Sato F.** 2002. Characterization of an *Arabidopsis thaliana* mutant with impaired *psbO*, one of two genes encoding extrinsic 33-kDa proteins in photosystem II. *The Plant Cell* **523,** 138–142.

**Murakami R, Ifuku K, Takabayashi A, Shikanai T, Endo T, Sato F.** 2005. Functional dissection of two *Arabidopsis* PsbO proteins. *FEBS Journal* **272,** 2165–2175.

**Murashige T, Skoog F.** 1962. A revised medium for rapid growth and bioassays with tobacco tissue cultures. *Physiologia Plantarium* **15,** 473–497.

**Murata N, Takahashi S, Nishiyama Y, Allakhverdiev SI.** 2007. Photoinhibition of photosystem II under environmental stress. *Biochimica et Biophysica Acta – Bioenergetics* **1767,** 414–421.

**Ögren E, Evans JR.** 1993. Photosynthetic light-response curves. I. The influence of $CO_2$ partial pressure and leaf inversion. *Planta* **189,** 182–190.

**Oguchi R, Douwstra P, Fujita T, Chow WS, Terashima I.** 2011. Intra-leaf gradients of photoinhibition induced by different color lights: implications for the dual mechanisms of photoinhibition and for the application of conventional chlorophyll fluorometers. *New Phytologist* **191,** 146–159.

**Ohad I, Kyle DJ, Arntzen CJ.** 1984. Membrane protein damage and repair: removal and replacement of inactivated 32-kilodalton polypeptides in chloroplast membranes. *Journal of Cell Biology* **99,** 481–485.

**Oxborough K, Baker NR.** 1997a. An instrument capable of imaging chlorophyll a fluorescence from intact leaves at very low irradiance and at cellular and subcellular levels of organization. *Plant, Cell and Environment* **20,** 1473–1483.

**Oxborough K, Baker NR.** 1997b. Resolving chlorophyll *a* fluorescence images of photosynthetic efficiency into photochemical and non-photochemical components – calculation of *qP* and *Fv'/Fm'* without measuring *Fo'*. *Photosynthesis Research* **54,** 135–142.

**Pengelly JJL, Sirault XRR, Tazoe Y, Evans JR, Furbank RT, von Caemmerer S.** 2010. Growth of the $C_4$ dicot *Flaveria bidentis*:

photosynthetic acclimation to low light through shifts in leaf anatomy and biochemistry. *Journal of Experimental Botany* **61,** 4109–4122.

**Pfannschmidt T, Nilsson A, Allen JF.** 1999. Photosynthetic control of chloroplast gene expression. *Nature* **397,** 625–628.

**Porra RJ, Thompson WA, Kriedemann PE.** 1989. Determination of accurate coefficients and simultaneous equations for assaying chlorophylls *a* and *b* extracted with four different solvents: verification of the chlororophyll standards by atomic absorption spectroscopy. *Biochimica et Biophysica Acta* **975,** 384–394.

**Price GD, von Caemmerer S, Evans JR, Siebke K, Anderson JM, Badger MR.** 1998. Photosynthesis is strongly reduced by antisense suppression of chloroplastic cytochrome *bf* complex in transgenic tobacco. *Australian Journal of Plant Physiology* **25,** 445–452.

**Price GD, Yu JW, von Caemmerer S, Evans JR, Chow WS, Anderson JM, Hurry V, Badger MR.** 1995. Chloroplast cytochrome *b6/f* and ATP synthase complexes in tobacco: transformation with antisense RNA against nuclear-encoded transcripts for the Rieske FeS and ATPδ polypeptides. *Australian Journal of Plant Physiology* **22,** 285–297.

**Raines C.** 2003. The Calvin cycle revisited. *Photosynthesis Research* **75,** 1–10.

**Rott M, Martins NdF, Thiele W, Lein W, Bock R, Kramer DM, Schöttler MA.** 2011. ATP synthase repression in tobacco restricts photosynthetic electron transport, $CO_2$ assimilation, and plant growth by overacidification of the thylakoid lumen. *The Plant Cell* **23,** 304–321.

**Ruuska SA, Andrews TJ, Badger MR, Hudson GS, Laisk A, Price GD, von Caemmerer S.** 1998. The interplay between limiting processes in $C_3$ photosynthesis studied by rapid-response gas exchange using transgenic tobacco impaired in photosynthesis. *Australian Journal of Plant Physiology* **25,** 859–870.

**Ruuska SA, Andrews TJ, Badger MR, Price GD, von Caemmerer S.** 2000. The role of chloroplast electron transport and metabolites in modulating rubisco activity in tobacco. Insights from transgenic plants with reduced amounts of cytochrome *b/f* complex or glyceraldehyde 3-phosphate dehydrogenase. *Plant Physiology* **122,** 491–504.

**Satoh K.** 1996. Introduction to the photosystem II reaction centre–Isolation and biochemical and biophysical characterisation. In: DR Ort, CF Yocum, ed.tors, *Oxygenic photosynthesis: the light reactions*. Dordrecht. Kluwer Academic, pp 193–211.

**Shimizu M, Kato H, Ogawa T, Kurachi A, Nakagawa Y, Kobayashi H.** 2010. Sigma factor phosphorylation in the photosynthetic control of photosystem stoichiometry. *Proceedings of the National Academy of Sciences, USA* **107,** 10760–10764.

**Stirling CM, Rodrigo VH, Emberru J.** 1993. Chilling and photosynthetic productivity of field grown maize (*Zea mays*); changes in the parameters of the light-response curve, canopy leaf $CO_2$ assimilation rate and crop radiation-use efficiency. *Photosynthesis Research* **38,** 125–133.

**Stockhaus J, Höfer M, Renger G, Westhoff P, Wydrzynski T, Willmitzer L.** 1990. Anti-sense RNA efficiently inhibits formation of the 10 kd polypeptide of photosystem II in transgenic potato plants: analysis of the role of the 10 kd protein. *The EMBO Journal* **9,** 3013–3021.

**Sundby C, McCaffery S, Anderson JM.** 1993. Turnover of the photosystem II D1 protein in higher plants under photoinhibitory and nonphotoinhibitory irradiance. *Journal of Biological Chemistry* **268,** 25476–25482.

**Takahashi S, Badger MR.** 2011. Photoprotection in plants: a new light on photosystem II damage. *Trends in Plant Science* **16,** 53–60.

**Takahashi S, Murata N.** 2008. How do environmental stresses accelerate photoinhibition? *Trends in Plant Science* **13,** 178–182.

**Terashima I, Evans JR.** 1988. Effects of light and nitrogen nutrition on the organization of the photosynthetic apparatus in spinach. *Plant and Cell Physiology* **29,** 143–155.

**Tyystjärvi E.** 2008. Photoinhibition of photosystem II and photodamage of the oxygen evolving manganese cluster. *Coordination Chemistry Reviews* **252,** 361–376.

**van Gorkom H, Schelvis J.** 1993. Kok's oxygen clock: what makes it tick? The structure of P680 and consequences of its oxidizing power. *Photosynthesis Research* **38,** 297–301.

**von Caemmerer S.** 2000. *Biochemical models of leaf photosynthesis*. Melbourne. CSIRO Publishing.

**von Caemmerer S, Farquhar GD.** 1981. Some relationships between the biochemistry of photosynthesis and the gas-exchange of leaves. *Planta* **153,** 376–387.

**Wollman F-A, Minai L, Nechushtai R.** 1999. The biogenesis and assembly of photosynthetic proteins in thylakoid membranes. *Biochimica et Biophysica Acta – Bioenergetics* **1411,** 21–85.

**Yamashita A, Nijo N, Pospisil P, Morita N, Takenaka D, Aminaka R, Yamamoto Y.** 2008. Quality control of photosystem II – reactive oxygen species are responsible for the damage to photosystem II under moderate heat stress. *Journal of Biological Chemistry* **283,** 28380–28391.

**Yamori W, Evans JR, Von Caemmerer S.** 2010. Effects of growth and measurement light intensities on temperature dependence of $CO_2$ assimilation rate in tobacco leaves. *Plant, Cell and Environment* **33,** 332–343.

**Yamori W, Nagai T, Makino A.** 2011a. The rate-limiting step for $CO_2$ assimilation at different temperatures is influenced by the leaf nitrogen content in several $C_3$ crop species. *Plant, Cell and Environment*, **34,** 764–777.

**Yamori W, Noguchi K, Kashino Y, Terashima I**. 2008**.** The role of electron transport in determining the temperature dependence of the photosynthetic rate in spinach leaves grown at contrasting temperatures. *Plant and Cell Physiology* **49,** 583–591.

**Yamori W, Noguchi K, Terashima I.** 2005. Temperature acclimation of photosynthesis in spinach leaves: analysis of photosynthetic components and temperature dependencies of photosynthetic partial reactions. *Plant, Cell and Environment* **28,** 536–547.

**Yamori W, Takahashi S, Makino A, Price GD, Badger MR, von Caemmerer S.** 2011b. The roles of ATP synthase and the cytochrome $b_6/f$ complexes in limiting chloroplast electron transport and determining photosynthetic capacity. *Plant Physiology* **155,** 9569–62.

**Yi X, McChargue M, Laborde S, Frankel LK, Bricker TM.** 2005. The manganese-stabilizing protein is required for photosystem II assembly/stability and photoautotrophy in higher plants. *Journal of Biological Chemistry* **280,** 16170–16174.